AUTOMATIC CONTROL SYSTEM FOR AN AIRCRAFT PLAN SUPERSONIC INLET WITH MOBILE PANEL

Alexandru Nicolae TUDOSIE, Mádálina Luciana PĂUNESCU

University of Craiova, Craiova, Romania (atudosie@elth.ucv.ro, madalina.paunescu92@yahoo.com)

DOI: 10.19062/2247-3173.2017.19.1.27

Abstract: *The paper deals with a plan supersonic inlet with external compression and mobile panel and studies its control system, based on the second oblique shock-wave positioning and its total pressure ratio recovery. The system's gas-dynamic conditioning and control criteria are determined. The author has established the system's non-linear mathematical model and, finally, the linear non-dimensional model; the block diagram with transfer functions description, based on the above-mentioned models was also provided. Some simulations, concerning the system's stability and quality were performed; furthermore, some conclusions and comment concerning system's time behavior were issued.*

Keywords: *inlet, supersonic, Mach number, control law, angle, shock-wave, pressure, step input.*

1. INTRODUCTION

The possibilities of the engine's supersonic inlet's control, in order to assure the balance of the engine's necessary air flow rate and the inlet's delivered air flow rate, are the flow section area's control by the spike's positioning or by the inlet's inner cowl's positioning [2, 3, 12], as well as the inner minimum cross-section area control by the inner diaphragm's positioning [11]; the controlled parameter should be the shock-wave's total pressure ratio (also known as "inlet's inner perfection co-efficient" or pressure recovery co-efficient), as well as the minimum section pressure ratio. One can observe that the system assures the shock wave's pressure ratio's preservation through the shock wave's positioning, based on the feed back error's canceling. Formally, a kind of control system's diagram is presented in Fig.1, similar to the one in [11].

The inlet in Fig. 2 (similar to the one studied in [13] and [14]) has a spike with two disturbance surfaces, which are generating two conic shock waves, so the inner air flow inside the intake remains supersonic; the first body's disturbance surface is a fixed-one, but the second one has a variable-angle mobile panel.

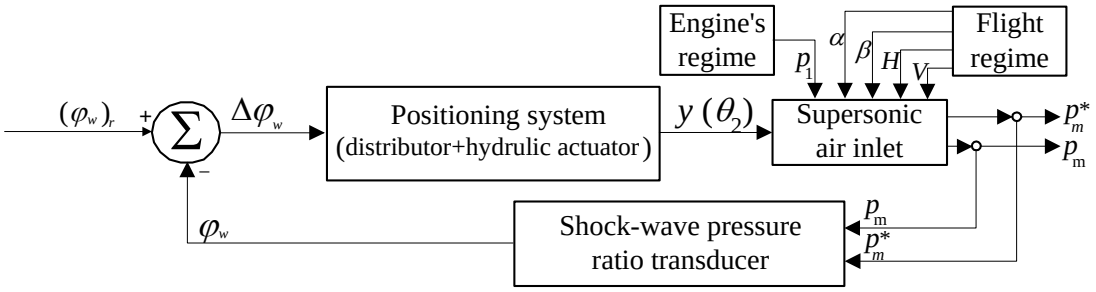

FIG. 1. Supersonic inlet control system's formal block diagram

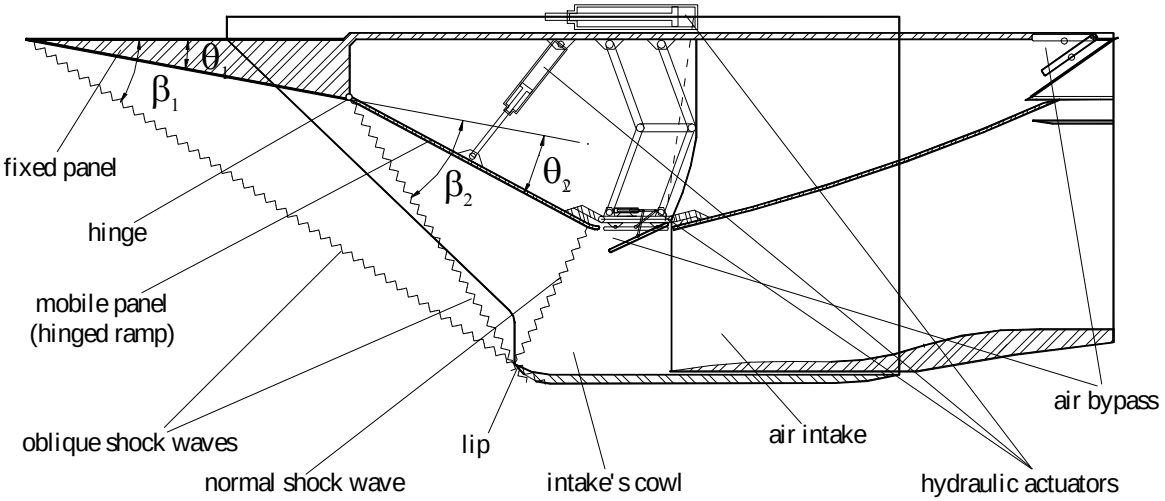

FIG. 2. Supersonic inlet with mobile panel "2+1"-type [13]

The air flow's speed is decreasing, but the leap supersonic/subsonic is realized by a normal shock wave in the front of the intake (attached to intake's lip at nominal regime, when Mach number in front of the inlet is the "design Mach number" and engine's rotational speed is the nominal one- the maximum or the cruise maximum value) [9]. This is the way to assure the gas-dynamic stability against any flow disturbances and also the inlet's "activation" during transonic flights.

2. CONTROL SYSTEM'S DESCRIPTION

The architecture of the automatic control system is depicted in Fig. 3. It consists of a mobile panel (of the inlet's spike) with pressure intakes, a pressure sensor (with two capsules, one for the total pressure, the other for the static pressure) and a hydraulic actuator with a slide-valve distributor. System's main parts are identified in Fig. 3.

Pressure intakes are positioned in order to measure the mean total pressure p_m^* and the mean static pressure p_m behind the second oblique shock-wave. Pressures ratio φ_w, from aerodynamic and thermodynamic points of view, is a function of the Mach number behind the second shock wave M_3, as follows:

$$\varphi_w = \frac{p_m^*}{p_m} = \left(1 + \frac{\chi - 1}{2} M_3^2\right)^{\frac{\chi}{\chi - 1}}. \tag{1}$$

Inlet's control law, with respect to the flight regime, as determined in [15], has a form depending on the Mach number in front of the inlet M_1. Thus, Mach number(s) behind the shock-wave(s) (M_2 and/or M_3) are depending themselves on M_1. One may affirm that the pressure ratio behind the oblique shock-wave(s) should be preserved, which involves the panel repositioning with respect to the Mach number.

The inlet operates both as "1+1" and as "2+1" external compression device; for low values of Mach number M_1, the mobile panel is kept on its initial position (as an extension of the fixed panel of the inlet); after $M_1 = 1.8$ the mobile panel will be positioned with respect to the flight Mach number.

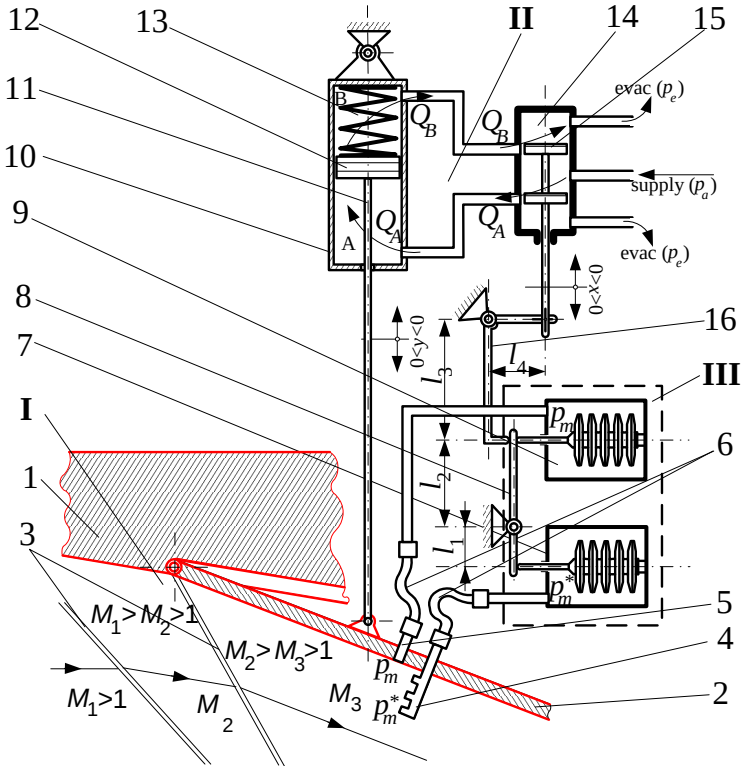

System's main parts:

I-supersonic inlet;
II-actuator;
III-pressure sensor;

1-inlet's spike; 2-spike's hinged mobile panel; 3-oblique shock-waves; 4-total pressure intakes ramp; 5-static pressure intake; 6-flexible pipes; 7-total pressure sensor (capsels); 8-pressure sensor's lever; 9-static pressure sensor (capsels); 10-hydraulic actuator; 11-actuator's rod; 12-actuator's piston; 13-actuator's spring; 14-distributor; 15-distributor's slide-valve; 16-rocking lever.

FIG. 3. Automatic control system architecture

Modifying the Mach number means modifying the pressure balance, as well as pressure ratio; when the mobile panel is repositioned, pressure ratio should be restored, in order to assure the same position of the second oblique shock-wave. Positioning law is a non-linear one, but it could be linearised, accepting a mobile panel positioning error and, obviously, a better correlation with the complementary control law (which means the inlet cowl's displacement).

3. SYSTEM'S MATHEMATICAL MODEL

3.1. Non-linear equation system. The system's mathematical model consists of the motion equations for its main parts: static and total pressure's transducer, hydraulic distributor and actuator. These equations are, as follows:

a) pressure ratio's transducer's equation:

$$S_{a1} l_1 p_m^* - S_{a2} l_2 p_m - \frac{l_2 l_4}{l_3}\left(m\frac{\mathrm{d}^2 x}{\mathrm{d}t^2} + \xi\frac{\mathrm{d}x}{\mathrm{d}t}\right) - \left(k_{r1} l_1 + k_{r2} l_2\right)x = 0, \tag{2}$$

where k_{r1}, k_{r2} – transducer's capsule's elastic constants; m – mobile rod and accessories mass; ξ – viscous friction co-efficient; l_1, l_2 – transducer's lever arms length; l_3, l_4 – transducer's rocking lever arms length; S_{a1}, S_{a2} – aneroid capsules surface areas (usually considered as equal $S_{a1} = S_{a2} = S_a$); x – distributor's slide-valve's displacement;

b) actuator's and distributor's equations:

$$Q_A = \mu_a L_d x \sqrt{\frac{2}{\rho_{hf}}} \sqrt{p_a - p_A}\,, \tag{3}$$

$$Q_B = \mu_a L_d x \sqrt{\frac{2}{\rho_{hf}}} \sqrt{p_B - p_e}\,, \tag{4}$$

$$Q_A = S_p \frac{\mathrm{d}(y_r - y)}{\mathrm{d}t} + \beta_{hf} V_{A0} \frac{\mathrm{d}p_A}{\mathrm{d}t} \tag{5}$$

$$Q_B = S_p \frac{\mathrm{d}(y_r + y)}{\mathrm{d}t} - \beta_{hf} V_{B0} \frac{\mathrm{d}p_B}{\mathrm{d}t}, \tag{6}$$

$$S_p (p_A - p_B) = m_p \frac{\mathrm{d}^2(y + y_r)}{\mathrm{d}t^2} + \xi_f \frac{\mathrm{d}(y + y_r)}{\mathrm{d}t} + k_{ea}(y_r + y + y_0), \tag{7}$$

where Q_A, Q_B – hydraulic fluid's flow rates; μ_a – flow rate co-efficient; L_d – distributor's orifice's width; p_A, p_B – actuator's chambers' pressures; y – actuator's rod's displacement; V_A, V_B – transducer's chambers volume; β_{hf} – hydraulic fluid's compressibility co-efficient; k_{ea} – actuator's spring's elastic constant; m_p – actuator's mobile rod and accessories mass; ξ_f – viscous friction co-efficient; p_a – hydraulic fluid supplying pressure; p_e – fluid's pressure in the low pressure circuit (considered negligible, because of its small value, comparing with p_A and p_B).

System's non-linear mathematical model is described by the equations (2) to (7).

3.2. Linearised mathematical model. The above determined non-linear equation system can be linearised using the small perturbation method, considering formally any variable X as $X = X_0 + \Delta X$ and $\overline{X} = \frac{\Delta X}{X_0}$, where ΔX – deviation, X_0 – steady state regime's value and $\overline{X}$ – non-dimensional deviation. One can also make some supplementary hypothesis, considering that the system works nearby a steady state position, thus $V_{30} \approx V_{40} = V_0$, $p_{30} = p_{40} + \frac{k_{ea} y_0}{S_p}$, $p_{40} \approx p_{30} = \frac{p_a - p_e}{2}$.

Introducing (3) into (5) and (4) into (6), than adding (4) to (6) it results:

$$S_{a1} l_1 p_m^* - S_{a2} l_2 p_m - \frac{l_2 l_4}{l_3}\left(m \frac{\mathrm{d}^2 x}{\mathrm{d}t^2} + \xi \frac{\mathrm{d}x}{\mathrm{d}t}\right) - (k_{r1} l_1 + k_{r2} l_2) x = 0, \tag{8}$$

$$l_1 \Delta p_m^* - l_2 \Delta p_m = \frac{k_{r1} l_1 + k_{r2} l_2}{S_a}\left(T_x^2 \frac{\mathrm{d}^2}{\mathrm{d}t^2} \Delta x + 2 T_x \omega_0 \frac{\mathrm{d}}{\mathrm{d}t} \Delta x + \Delta x\right), \tag{9}$$

$$\beta_{hf}V_0\frac{\mathrm{d}}{\mathrm{d}t}\left(\Delta p_A-\Delta p_B\right)+k_{Ap}\left(\Delta p_A-\Delta p_B\right)=2k_{Ax}\Delta x-2S_p\frac{\mathrm{d}}{\mathrm{d}t}\Delta y\,, \tag{10}$$

$$\Delta p_A-\Delta p_B=\frac{k_{ea}}{S_p}\left(T_y^2\frac{\mathrm{d}^2}{\mathrm{d}t^2}\Delta y+2T_y\omega_0\frac{\mathrm{d}}{\mathrm{d}t}\Delta y+\Delta y\right), \tag{11}$$

where

$$k_{Ax}=\mu_a L_d\sqrt{\frac{p_a-p_e}{\rho_{hf}}},\ T_x=\sqrt{\frac{ml_2l_4}{\left(k_{r1}l_1+k_{r2}l_2\right)l_3}},\ 2T_x\omega_0=\frac{\xi\, l_2l_4}{\left(k_{r1}l_1+k_{r2}l_2\right)l_3},\ T_y=\sqrt{\frac{m_p}{k_{ea}}},$$
$$2T_y\omega_0=\frac{\xi_f}{k_{ea}},\ k_{Ap}=\mu_a L_d x_0\sqrt{\frac{1}{\rho_{hf}\left(p_a-p_e\right)}}. \tag{12}$$

Noting also

$$k_{xS}=\frac{S_a}{k_{r1}l_1+k_{r2}l_2},k_{px}=\frac{2k_{Ax}}{k_{Ap}},\ \tau_{py}=\frac{2S_p}{k_{Ap}},\tau_{Ap}=\frac{\beta_{hf}V_0}{k_{Ap}},\ k_{py}=\frac{S_p}{k_{ea}}, \tag{13}$$

then, applying the Laplace transforming to the above-presented (8) to (11) equations, one can describe the system by a block diagram, as shown in Fig. 4.

3.3. System non-dimensional linear model and transfer function. Based on the equation system, as well as on the block diagram in fig. 4, one can observe that the model and the transfer functions in the block diagram may be simplified if one assume some new hypothesis: 1) the inertial effects are very small, because of the reduced masses *m* and m_p, so the time constants T_x and T_y can be considered as null; 2) viscous friction effects can also be neglected, so all the terms in the above equations containing ξ_f or ξ as multipliers are becoming null too; 3) hydraulic fluid's compressibility is practically null, so the terms where β_{hf} is involved become also null (see τ_{Ap}).

Consequently, the new form of the system's mathematical model becomes

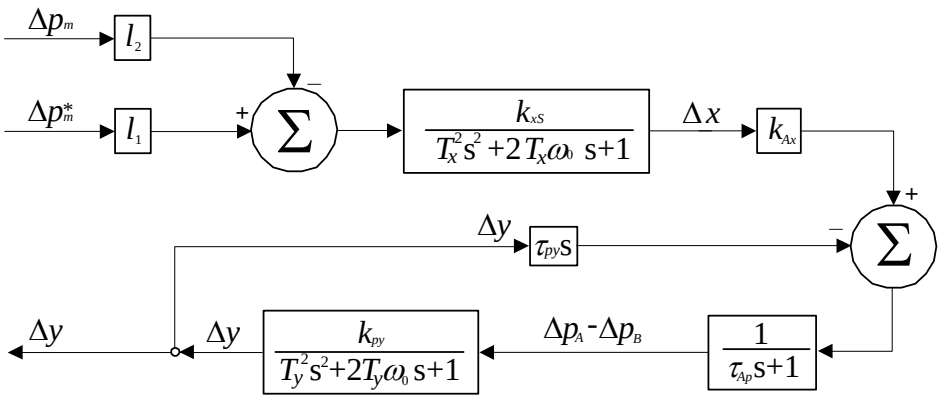

FIG. 4. System's block diagram

$$k_{mt}\overline{p_m^*}-k_m\overline{p_m}=\bar{x} \tag{14}$$

$$k_x\bar{x}-\tau_y s\bar{y}=(\tau_{Ap}s+1)(\overline{p_A}-\overline{p_B})\approx(\overline{p_A}-\overline{p_B}), \tag{15}$$

$$\bar{y}=k_y(\overline{p_A}-\overline{p_B}), \tag{16}$$

with the annotations

$$k_{mt}=\frac{l_1k_{xS}p_{m0}^*}{x_0}, k_m=\frac{l_2k_{xS}p_{m0}}{x_0}\approx k_{mt}, k_x=\frac{k_{px}x_0}{p_{A0}}, \tau_y=\frac{\tau_{py}y_0}{p_{A0}}, k_y=\frac{k_{py}p_{A0}}{y_0}. \tag{17}$$

The simplified block diagram is presented in Fig. 5 and the system's restraint model has the following form:

$$k_xk_y\left(k_{mt}\overline{p_m^*}-k_m\overline{p_m}\right)=(k_y\tau_y s+1)\bar{y}, \tag{18}$$

$$\bar{y}=\frac{k_xk_y}{(k_y\tau_y s+1)}\left(k_{mt}\overline{p_m^*}-k_m\overline{p_m}\right)=\frac{k}{(\tau s+1)}\left(k_{mt}\overline{p_m^*}-k_m\overline{p_m}\right). \tag{19}$$

that means a first order system's transfer function, where the time constant τ and the gain co-efficient k are

$$\tau=k_y\tau_y=\frac{2S_p^2\sqrt{\rho_{hf}(p_a-p_e)}}{k_{ea}\mu_aL_dx_0}, \tag{20}$$

$$k=k_xk_y=\frac{2S_p(p_a-p_e)}{k_{ea}y_0}. \tag{21}$$

System's transfer functions are

$$H_{mt}(s)=\frac{k_xk_yk_{mt}}{(k_y\tau_y s+1)}\overline{p_m^*} \tag{22}$$

$$H_m(s)=-\frac{k_xk_yk_m}{(k_y\tau_y s+1)}\overline{p_m}. \tag{23}$$

3.4. Equivalent form of the mathematical model. Based on some considerations, one can obtain a new form of the mathematical model and of system's transfer function, if one make the observation that pressure's ratio $\varphi_w = \frac{p_m^*}{p_m}$ deviation $\Delta\varphi_w$, as well as it non-dimensional deviation $\overline{\varphi}_w = \frac{\Delta\varphi_w}{\varphi_{w0}}$ may be expressed as:

$$\Delta\varphi_w = \frac{\Delta p_m^* p_m - p_m^* \Delta p_m}{p_m^2} = \frac{\Delta p_m^*}{p_m} - \Delta p_m \frac{p_m^*}{p_m^2}, \tag{24}$$

$$\overline{\varphi}_w = \frac{\Delta\varphi_w}{\varphi_{w0}} = \frac{\frac{\Delta p_m^*}{p_{m0}} - \Delta p_m \frac{p_{m0}^*}{p_{m0}^2}}{\frac{p_{m0}^*}{p_{m0}}} = \overline{p}_m^* - \overline{p}_m. \tag{25}$$

Consequently, the left member of Eq. (18) becomes

$$k_x k_y \left(k_{mt}\overline{p}_m^* - k_m \overline{p}_m\right) = k_x k_y k_{mt}\left(\overline{p}_m^* - \overline{p}_m\right) = k_x k_y k_{mt}\overline{\varphi}_w, \tag{26}$$

so, considering the above mentioned annotations, a new equivalent form of the simplified mathematical model will be issued, as follows

$$k_x k_y k_{mt}\left(\overline{\varphi}_r - \overline{\varphi}_w\right) = \left(k_y \tau_y \mathrm{s} + 1\right)\overline{y}, \tag{27}$$

where the new term in the above determined equation is $\overline{\varphi}_r$ – the preset reference value of the pressure ratio, given by

$$\overline{\varphi}_r = \frac{p_{m0}^3 l_4 \left(S_a p_{m0} - l_3 k_{r1}\right) l_3}{\left(l_3 k_{r2} - l_3 k_{r1} + S_a p_{m0}\right)^2 S_a \left(p_{m0}^*\right)^2}. \tag{28}$$

4. SYSTEM'S STABILITY AND QUALITY

Since transfer functions expressions are first order, as far as one chooses appropriate values for the system's geometric parameters, the above-studied system should be always a stabile one. The condition of stability ($k_y \tau_y$ strictly positive) is identically fulfilled if one chooses the values of the lever arms as

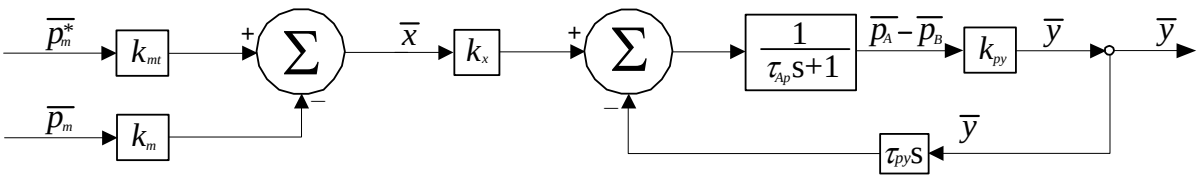

FIG. 5. System's simplified block diagram with transfer functions

$$l_1 = \frac{S_a p_{m0}^2 l_3}{p_{m0}^* \left(l_3 k_{r2} - l_3 k_{r1} + S_a p_{m0}\right)},\ l_2 = \frac{S_a p_{m0}^2 \left(S_a p_{m0} - l_3 k_{r1}\right)}{p_{m0}^* l_3 k_{r2} \left(l_3 k_{r2} - l_3 k_{r1} + S_a p_{m0}\right)}. \tag{29}$$

Moreover, if one chooses the aneroid capsules to have identical geometric shape and dimensions $\left(S_{a1} = S_{a2} = S_a, k_{r1} = k_{r2} = k_r\right)$, the above values of the lever arms become

$$l_1 = \frac{p_{m0}}{p_{m0}^*} l_3,\ l_2 = \frac{p_{m0}\left(S_a p_{m0} - l_3 k_r\right)}{p_{m0}^* k_r} \frac{l_4}{l_3}. \tag{30}$$

Based on the above presented mathematical model and coefficient values, some simulations were performed, regarding system's output $\bar{y}$ behavior as time response, considering both situations of step inputs: a) step input of $\bar{p}_m^*$ and constant $\bar{p}_m$, respectively b) step input of $\bar{p}_m$ and constant $\bar{p}_m^*$. Results are graphically presented in Fig. 6 a) and b), for both of the studied situations; the curves are represented with continuous line.

In order to improve system's behavior, a rigid feedback between the actuator and the distributor may be used; obviously, the presence of this feedback modifies system's mathematical model and transfer function. First of all, considering feedback's gain as $\rho_s = \frac{y_0}{x_0}\frac{l_y}{l_x}$ (where l_x, l_y are feedback's lever's arms length), one obtains new forms for Eqs. (10) and (15), as follows:

$$\beta_{hf} V_0 \frac{\mathrm{d}}{\mathrm{d}t}\left(\Delta p_A - \Delta p_B\right) + k_{Ap}\left(\Delta p_A - \Delta p_B\right) = 2k_{Ax}\Delta x - 2k_{Ax}\frac{l_y}{l_x}\Delta y - 2S_p \frac{\mathrm{d}}{\mathrm{d}t}\Delta y, \tag{31}$$

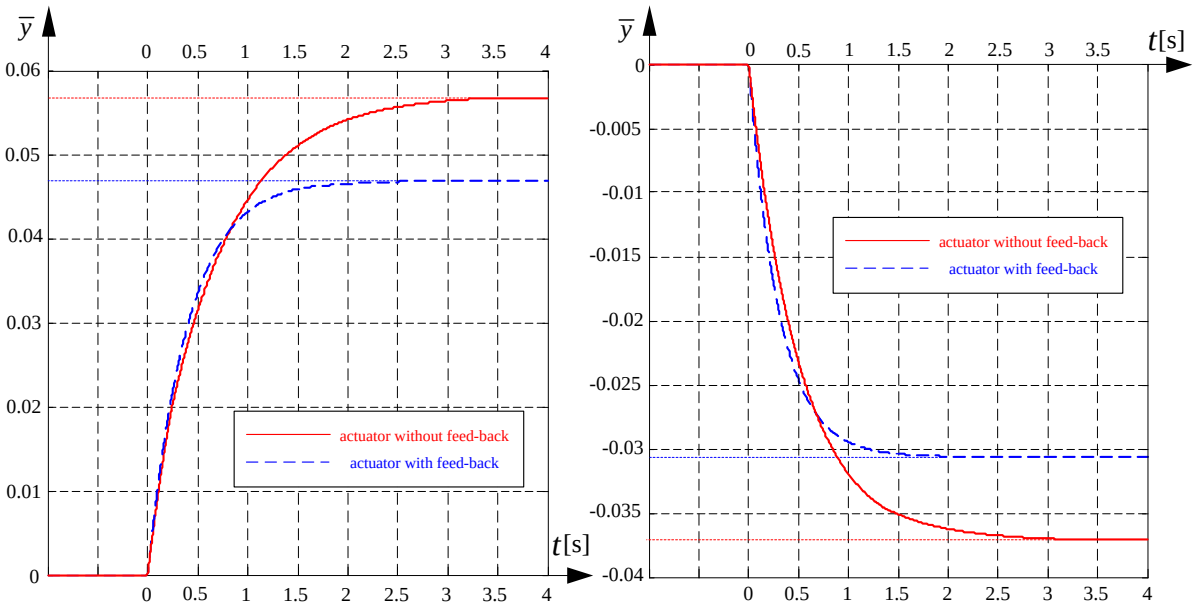

a) step input for $\bar{p}_m^*$ and constant $p_m\left(\bar{p}_m = 0\right)$ b) step input for $\bar{p}_m$ and constant $p_m^*\left(\bar{p}_m^* = 0\right)$

FIG. 6. System's step response for different step inputs

$$k_x\bar{x}-(\tau_y s+\rho_s)\bar{y}=(\tau_{Ap}s+1)(\overline{p_A}-\overline{p_B})\approx(\overline{p_A}-\overline{p_B}), \tag{32}$$

so, eventually, the new mathematical model becomes

$$\bar{y}=\frac{k_xk_y}{(k_y\tau_y s+k_y\rho_s+1)}\left(k_{mt}\overline{p_m^*}-k_m\overline{p_m}\right)=\frac{k_1}{(\tau_1 s+1)}\left(k_{mt}\overline{p_m^*}-k_m\overline{p_m}\right), \tag{33}$$

where new values of the time constant and of the gain are becoming smaller, as their next forms are proving:

$$\tau_1=\frac{k_y}{k_y\rho_s+1}\tau_y,\quad k_1=\frac{k_xk_y}{k_y\rho_s+1}. \tag{34}$$

Based on the new mathematical model, a similar simulation was performed, for both of step input situations. Results are graphically presented in Fig. 6 a) and b), for both of the studied situations, but the curves corresponding to the new model are represented with dashed line.

CONCLUSIONS

Supersonic inlets' automation is one of the most important issues in aircraft engineering. There are a lot of control laws for such inlets, each one of them having its own form and also its own motivation.

In this paper authors have studied a plan supersonic inlet with mobile ramp, as controlled object; an automatic control system was described and mathematically modeled. As controlled parameter the system had the mobile panel's position (more specific: its position angle measured with respect to the spike's fixed panel direction), and as control parameter one has chosen the pressure ratio through the second oblique shock-wave (which is proportional to the flow's Mach number behind this shock).

Control system's most important element is the pressure transducer, which should realize both the sensing task, as well as the comparing with the preset pressure ratio value, imposed by the lever's arm's length choice.

System's mathematical model was linearised and brought to a dimensionless form, in order to be used for studies; one has obtained (after appropriate simplifying) a first order system and its transfer functions were also determined, with respect to the chosen inputs (the total pressure and the static pressure).

From the stability condition the lengths of pressure system's lever arms were determined. An appropriate choosing of pressure system's lever's length assures (even in the phase of control system's pre-design) control system's stability.

Some simulation were performed, for system's time behavior studying, from its output $\bar{y}$ point of view. In fact, y – displacement versus Mach number is non-linear, but it follows properly the control law. The authors have studied two cases, for both pressure (total and static pressure) step inputs. Simulation results, consisting of mobile panel's displacement for both chosen inputs, were graphically represented in Fig. 6. One can observe that in any case, the system has an asymptotically stabile behavior.

For a system with a simple actuator (without inner feedback), the results for both of studied cases show that the system has appropriate stabilization time (around 3.2 seconds for both of cases a) and b)) and, meanwhile, it has static errors (a positive one, 5.5% for $\overline{p}_m^*$ -step input, respectively a negative one, -3.7% for $\overline{p}_m$ -step input).

In order to improve system's time behavior, one has choose to use an actuator with inner feedback (after its rod displacement, as studied in [14]), instead of the basic actuator presented in Fig. 3; as result, system's step response was improved, but not essentially. Thus, the stabilization times were reduced (from 3.2 seconds to $2.0 \div 2.5$ seconds), which means that the intensity of the command signal was diminished; meanwhile, system's static error were also reduced, but not essentially: from 5.5% to 4.7 % for $\overline{p}_m^*$ -step input, respectively from -3.7% to -3.1 % for $\overline{p}_m$ -step input.

The paper has studied only the main control system of the inlet, the one that acts over the mobile panel; obviously, the paper could be extended with the study of the complementary control law implementation, which means another control system (for the intakes cowl position) which should compulsory operate correlated with the main control system. Moreover, an embedded control system (with correlated architectures) could be described and studied.

REFERENCES

[1] Abraham, R. H. *Complex dynamical systems*. Aerial Press, Santa Cruz, California, 1986;

[2] Aron, I., Tudosie, A., Hydromechanical System For The Supersonic Air Inlet's Channel's Section Control, pp. 266-269, *Proceedings of the International Conference on Applied and Theoretical Electricity*, Craiova, 2000;

[3] Lungu, R., Tudosie, A., Hydromechanical System For The Supersonic Air Intake's Central Corp's Positioning, pp. 266-269, *Proceedings of the International Conference on Applied and Theoretical Electricity*, Craiova, 2000;

[4] Lungu, R. *Flight apparatus automation*. Publisher Universitaria, Craiova, 2000;

[5] Mattingly, J. D. *Elements of gas turbine propulsion*. McGraw-Hill, New York, 1996*;*

[6] Stevens, B.L., Lewis, E. *Aircraft control and simulation*, John Willey Inc. N. York, 1992;

[7] Pimsner, V. *Air-breathing jet engines. Processes and characteristics*. Didactical and Pedagogical Publisher, Bucharest, 1984;

[8] Pimsner, V., Berbente, C. and others, *Flows in turbo-machinery*, Tehnica Publishing Bucharest, 1986, ISBN 973-165-4-17;

[9] Rotaru, C., Sprintu, I. State Variable Modeling of the Integrated Engine and Aircraft Dynamics, pp. 889-898, *Proceedings of ICNPAA 2014 (10th International Conference On Mathematical Problems In Engineering, Aerospace And Sciences)*, Narvik, Norway, 15-18 July, 2014.

[10] Seddon, J. and Goldsmith, E. L. *Intake Aerodynamics, 2nd edition*, AIAA Education Series, 1999.

[11] Tudosie, A. Supersonic Air Inlet's Control System Based On The Inner Normal Shock Wave's Position Stabilisation, pp. 342-349, *Proceedings of International Conference on Military Technologies ICMT 2007*, University of Defense, Brno, Czech Republic, 3-5th May, 2007;

[12] Tudosie, A. Hydromechanical System for the Supersonic Air Inlet's Central Corp's Positioning, pp. 270-275, *Proceedings of International Conference on Applied and Theoretical Electricity ICATE 2000*, Craiova, 25-26th May, 2000.

[13] Tudosie, A., Dragan, A. Rectangular supersonic air inlet with movable ramp, pp. 453-458, *Proceedings of International Conference on Applied and Theoretical Electricity ICATE 2002*, Craiova, 17-18th Oct. 2002.

[14] Tudosie, A. *Aerospace propulsion systems automation*, Inprint of University of Craiova, 2005.

[15] Tudosie, A. Control Laws For An Aircraft Supersonic Inlet With Mobile Panel, *unpublished*, 2017.